# Supporting information for Charge-neutral constant pH molecular dynamics simulations using a parsimonious proton buffer

Serena Donnini,[†] R. Thomas Ullmann,[‡] Gerrit Groenhof,[*,¶] and Helmut Grubmüller[*,‡]

† *Nanoscience Center and Department of Biological and Environmental Sciences, University of Jyväskylä, P.O. Box 35, 40014 Jyväskylä, Finland.*

‡*Department of Theoretical and Computational Biophysics, Max Planck Institute for Biophysical Chemistry, Am Faßberg 11, 37077 Göttingen, Germany.*

¶ *Nanoscience Center and Department of Chemistry, University of Jyväskylä, P.O. Box 35, 40014 Jyväskylä, Finland.*

E-mail: gerrit.xgroenhof@jyu.fi; hgrubmu@gwdg.de

This Supporting Information contains the force field parameters for the hydronium ions, the parameters of the biasing potential $U^{\mathrm{dwp}}$, and the coefficients of the polynomial fits to $\Delta G^{FF}$, illustrates the dynamics of deprotonation of a single titratable site with different heights of the outer walls of the potential $U^{\mathrm{dwp}}$, and shows the charge conservation of the constraint approach, and the convergence of the protonation macrostate free energies in our simulations at $\mathrm{pH} = \mathrm{p}K_{\mathrm{a}}$.

## Hydronium force field parameters

Table S1 list the atomic charges[1] and atom types of the hydronium ion in the protonated and deprotonated states. Atom types are defined in GROMOS96 53A6[2].

Table S1

| | protonated | | deprotonated | |
|---|---|---|---|---|
| atom | atom type | atom charge | atom type | atom charge |
| OW | OW | -0.590 | OW | -0.834 |
| HW1 | H | 0.000 | H | 0.417 |
| HW2 | H | 0.000 | H | 0.417 |
| H31 | H | 0.530 | H | 0.000 |
| H32 | H | 0.530 | H | 0.000 |
| H33 | H | 0.530 | H | 0.000 |

## Biasing potential parameters

Table S2 lists the parameters of the double well potential $U^{\text{dwp}}$ (equation 3 in main text) for different heights of the barrier $h$ and outer walls $w$.

Table S2

| | w=50 | | | w=200 | | |
|---|---|---|---|---|---|---|
| parameter | h=4 | h=7 | h=10 | h=0 | h=4 | h=7 |
| k | 2.530 | 4.396 | 6.267 | 0 | 2.553 | 4.417 |
| a | 0.03371 | 0.04214 | 0.05130 | 0.04764 | 0.034041 | 0.04208 |
| b | 0.004491 | 0.002717 | 0.001411 | -0.09706 | 0.005238 | 0.002957 |
| r | 21.428 | 21.428 | 21.428 | 16.458 | 16.458 | 16.458 |
| m | 0.1078 | 0.1078 | 0.1078 | 0.1507 | 0.1507 | 0.1507 |
| d | 2.0 | 3.5 | 5.0 | 0.0 | 2.0 | 3.5 |

## $\Delta G^{FF}$ parameters

Table S3 and Table S4 list the coefficients of the 4th order polynomials (with $a_0 = 0$), which are fitted to the free energy profiles from the reference deprotonation free energy simulations of the four acetic acids (ACE1 to ACE4) and of the buffer sites, respectively. In Table S4, the coefficients of four independent buffer sites H3OB1 to H3OB4, and of two (BUFF-2) and four (BUFF-4)

collective buffer sites are listed.

Table S3

| coefficient | ACE1 | ACE2 | ACE3 | ACE4 |
|---|---|---|---|---|
| $a_1$ | 38.744 | 34.623 | 37.154 | 46.992 |
| $a_2$ | -291.181 | -287.682 | -292.509 | -297.657 |
| $a_3$ | 14.8643 | 6.29767 | 15.232 | 25.532 |
| $a_4$ | -23.3225 | -18.2207 | -21.8173 | -26.585 |

Table S4

| | independent buffer sites | | | | collective buffer sites | |
|---|---|---|---|---|---|---|
| coefficient | H3OB1 | H3OB2 | H3OB3 | H3OB4 | BUFF-2 | BUFF-4 |
| $a_1$ | 600.403 | 598.507 | 589.269 | 596.562 | 1213.144 | 2418.130 |
| $a_2$ | -315.110 | -318.694 | -314.336 | -319.775 | -712.185 | -1412.910 |
| $a_3$ | 83.003 | 87.037 | 82.047 | 89.434 | 318.012 | 621.011 |
| $a_4$ | -57.506 | -60.309 | -57.470 | -61.271 | -201.150 | -395.837 |

To improve the fit to the deprotonation free energy profile of $\lambda^{\text{buffer}}$, which describes the concerted deprotonation of two or four buffer sites, we computed the remaining free energy profile by Boltzmann inverting the probability distributions of $\lambda^{\text{buffer}}$ from 100 constant pH MD simulations of 4.8 ns each, where the parameters for $\Delta G^{FF}(\lambda)$ in Table S4 were used. An additional correction potential ($U^{\text{corr}}(\lambda^{\text{buffer}})$) was subsequently obtained by fitting a polynomial to the resulting free energy profiles

$$U^{\text{corr}}(\lambda^{\text{buffer}}) = \sum_{i=0}^{11} a_i (\lambda^{\text{buffer}})^i \tag{1}$$

with coefficients $a_0 - a_{11}$ equal to 0.208, 1186.280, -630.636, 1534.315, -11608.188, 53371.505, -162806.183, 327143.042, -422351.459, 335308.568, -148666.625, and 28137.052, for BUFF-2, and 0.213, -71.400, 1005.680, -8851.012, 54700.106, -207551.111, 476446.483, -668636.626, 562485.676, -260681.004, 51156.249, and 0.000, for BUFF-4.

$U^{\text{corr}}(\lambda^{\text{buffer}})$ is applied to the interval $[0, 1]$ for BUFF-2 (two collective buffer sites), and to the interval $[-0.05, 1.05]$ for BUFF-4 (four collective buffer sites). In the BUFF-4 case, $U^{\text{dwp}}$ is added to $U^{\text{corr}}(\lambda^{\text{buffer}})$ to preserve the biasing potential $U^{\text{dwp}}$ beyond the interval $[0, 1]$.

## Verification of the adaptive biasing potential. Height of the outer walls

The steepness and the height of the outer walls of the adaptive biasing potential $U^{\mathrm{dwp}}$ (Equation 3, main text) must be large enough to prevent the $\lambda$ particle from escaping from the $[0, 1]$ interval. Here, two values of the height of the outer walls, $50$ kJ mol$^{-1}$ ($w = 50$) and $200$ kJ mol$^{-1}$ ($w = 200$), were tested on a single titratable site (hydronium) in explicit solvent. Figure S1 shows the $\lambda$ particle trajectories from 5 ns simulations. The distributions of the values of $\lambda$ are also shown next to the corresponding trajectories. Both trajectories sample the protonated ($\lambda = 0$) and deprotonated states ($\lambda = 1$), with $\langle\lambda\rangle = 0.53$ ($w = 50$) and $\langle\lambda\rangle = 0.54$ ($w = 200$), respectively. There is a slight increase (about $10\%$) in the transition rate, when increasing the height of the outer walls from 50 to 200 kJ mol$^{-1}$. In both cases, the $\lambda$ distribution is peaked at $0$ and $1$, respectively.

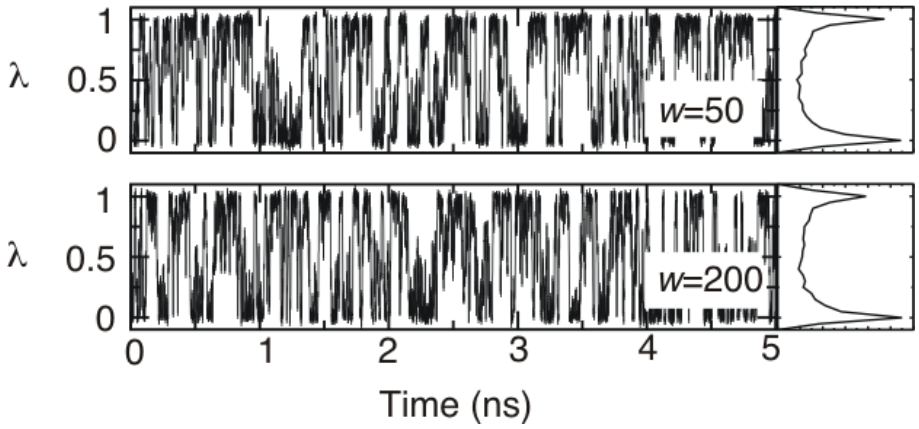


Figure S1: Dynamics of deprotonation of a single titratable site in explicit solvent with height of the outer walls of the biasing potential 50 kJ mol$^{-1}$ ($w = 50$) and 200 kJ mol$^{-1}$ ($w = 200$). Trajectories (left) and distributions (right) of the deprotonation coordinate $\lambda$ from 5 ns constant $\mathrm{pH}$ MD simulations. The height of the barrier of the biasing potential is 4 kJ mol$^{-1}$.

## Verification of the constraint

To verify that the constraint conserves the charge, Figure S2 reports the total charge of the system, from two constant pH MD simulations at $\mathrm{pH} = \mathrm{p}K_{\mathrm{a}}$, without constraint, and with constraint $c = 4$ (Equation 13, main text) and a single titration coordinate for four buffer sites (collective buffer

sites). In the simulation without constraint, the total charge of the four acetic acids fluctuates in the interval $[-4, 0]$ with $\langle q \rangle = -1.97$ $\mathrm{e}_\circ$. The total charge during the simulation with constraint and buffer sites is constant, with $q = 0$ $\mathrm{e}_\circ$, indicating that the constraint is satisfied. In this simulation, the charge of the four acetic acids ($\langle q \rangle = -1.98$ $\mathrm{e}_\circ$) is compensated by the charge of the buffer sites ($\langle q \rangle = 1.98$ $\mathrm{e}_\circ$).

Table S5 shows the average $\lambda$s from 100 constant pH MD simulations of 4.8 ns each at $\mathrm{pH} = \mathrm{p}K_\mathrm{a}$ without constraint, with constraint $c = 4$ and four independent buffer sites, and with constraint $c = 4$ and four collective buffer sites. The sum of the $\lambda$s and the deviation of the sum from the constraint $c = 4$ is also shown at the bottom of the table.

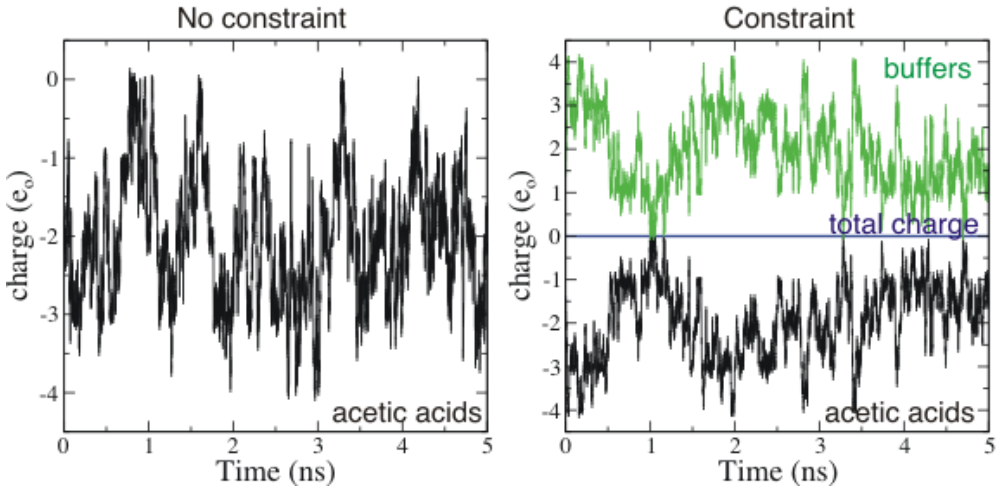


Figure S2: Total charge of the system from constant pH MD simulations of four acetic acids in explicit water at $\mathrm{pH} = \mathrm{p}K_\mathrm{a}$, without constraint (black) and with constraint $c = 4$ and four collective buffer sites (blue).

## Convergence of simulations

Figure S3 and Figure S4 show the cumulative protonation macrostate free energies of four acetic acids, obtained from constant pH MD simulations in explicit water at $\mathrm{pH} = \mathrm{p}K_\mathrm{a}$ without constraint, and with constraint $c = 4$ and four buffer sites described by a single titration coordinate $\lambda^{\mathrm{buffer}}$, respectively. The analytical solutions are indicated with orange broken lines. After sam-

Table S5: Average $\lambda$s from constant pH MD simulations of four acetic acids in explicit water at $\mathrm{pH} = \mathrm{p}K_\mathrm{a}$ without constraint, with constraint $c = 4$ and four independent buffer sites, and with constraint $c = 4$ and a single titration coordinate for the four buffer sites. The $\lambda_1 - \lambda_4$ describe deprotonation of the four acetic acids, respectively, and $\lambda^{\text{buffer}}$ is the titration coordinate describing converted deprotonation of the four buffer sites. The largest estimated error in the average $\lambda$ is $0.014$. At the bottom, deviation from the constraint $c = 4$ is reported.

| | no constraint | constraint and 4 independent buffer sites | constraint and collective buffer sites |
|---|---|---|---|
| $\langle\lambda_1\rangle$ | 0.499 | 0.508 | 0.499 |
| $\langle\lambda_2\rangle$ | 0.514 | 0.486 | 0.494 |
| $\langle\lambda_3\rangle$ | 0.498 | 0.495 | 0.498 |
| $\langle\lambda_4\rangle$ | 0.509 | 0.498 | 0.493 |
| $\langle\lambda^{\text{buffer}}\rangle$ | - | 0.521, 0.5149, 0.490, 0.486 | 0.504 |
| $\sum\langle\lambda_i\rangle$ | 2.020 | 4.000 | 4.000 |
| $\left\langle\left\lvert c - \sum\lambda_i\right\rvert\right\rangle$ | - | $8.343{\cdot}10^{-12}$ | $5.722{\cdot}10^{-12}$ |

pling for about 200 ns, the free energies of the macrostates have converged to their final values in the simulations.

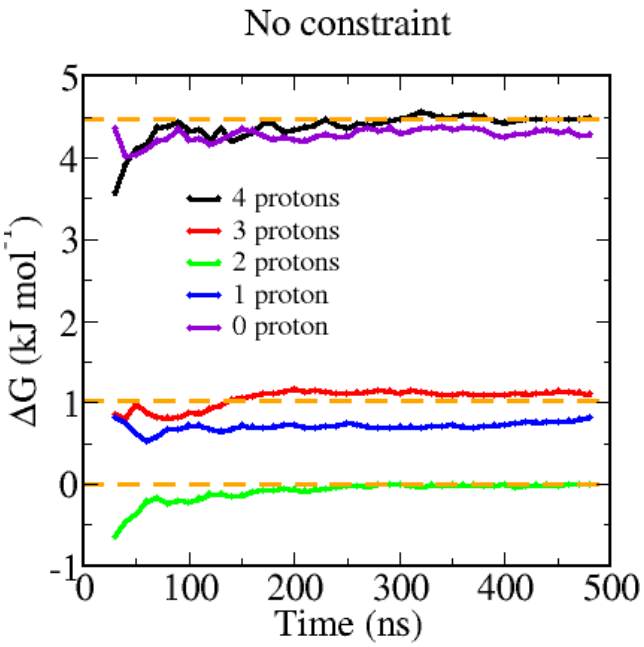


Figure S3: Cumulative free energy minima. In orange, from bottom to top, the analytical free energies of the two protons, one and three protons, and zero and four protons states, respectively.

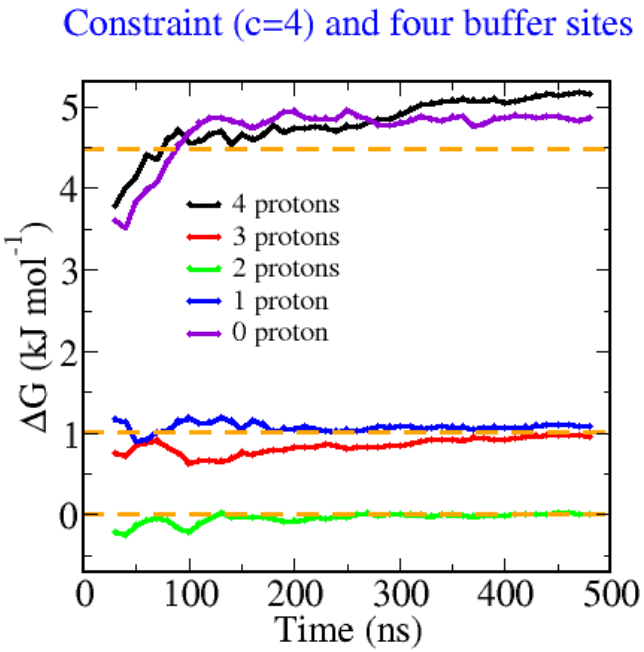


Figure S4: Cumulative free energy minima. In orange, from bottom to top, the analytical free energies of the two protons, one and three protons, and zero and four protons states, respectively.

# References

(1) Wolf, M. G.; Groenhof, G. *J. Comput. Chem.* **2014,** *35*, 657–671.

(2) Oostenbrink, C.; Villa, A.; Mark, A. E.; van Gunsteren, W. F. *J. Comput. Chem.* **2004,** *25*, 1656–1676.